DOI 10.1007/s11182-015-0587-5

Russian Physics Journal, Vol. 58, No. 7, November, 2015 (Russian Original No. 7, July, 2015)

SHAPE MEMORY EFFECT AND SUPERELASTICITY IN [001] SINGLE CRYSTALS OF Fe–Ni–Co–Al–Nb(B) FERROMAGNETIC ALLOY

Yu. I. Chumlyakov,[1] I. V. Kireeva,[1] O. A. Kuts,[1] M. Yu. Panchenko,[1] É. Karaka,[2] and H. J. Maier[3]

UDC 669.539.371:548.55

Shape memory effect (SME) and superelasticity (SE) during thermoelastic martensitic transformation (MT) from the FCC high-temperature γ-phase to the BCT α′-martensite are investigated in Fe – *28%* Ni – *17%* Co – *11.5%* Al – *2.5%* Nb (Nb) *and* Fe – *28%* Ni – *17%* Co – *11.5%* Al – *2.5%* Nb – *0.05%* B (NbB) *(at.%) single crystals oriented for tension along the [001] direction after aging at 973 K for 10 h. Non-equiaxial* (NiAl) *β-phase particles with thickness d and length l equal to 60–80 and 340–500 nm, respectively, and volume fraction f ≥ 3–5% are precipitated in* Nb *crystals during aging simultaneously with the* $(FeNiCo)_3(AlNb)$ *γ′-phase with sizes d = 12.5–16.5 nm. It is shown that precipitation of the β-phase with f ≤ 3–5% in the crystal volume does not reduce the crystal plasticity, and SME of 4.2% and SE up to 6.5% under loading are observed during thermoelastic γ–α′ MT in single crystals in a wide range of temperatures from 77 to 293 K. The β-phase is not detected in* NbB *crystals during aging. It is established that boron in* NbB *crystals slows down the aging processes: the γ′-phase particles have sizes 6.5–8 nm. The SME of 4.2% and SE up to 4.0% are observed in* NbB *crystals at temperatures from 77 to 243 K.*

Keywords: single crystals of iron-based alloys, thermoelastic martensitic transformation, shape memory effect, superelasticity, γ′- and β-phase particles.

INTRODUCTION

It is well known (for example, see [1–4]) that two ordered phases precipitate during aging in polycrystals of Fe–Ni–Co–Al–X (X = Ta, Nb, and Ti) iron-based alloys undergoing thermoelastic martensitic transformation (MT) from the FCC-phase (FCC (γ) is the face-centered cubic lattice) to BCT-martensite (BCT (α′) is the body-centered tetragonal lattice), namely, the γ′-phase with $L1_2$ structure precipitating inside the grain and the β-phase with $B2$ structure precipitating along the grain boundaries. Precipitation of the ordered γ′-phase with particle sizes 3–15 nm [1, 5–8] from the disordered initial phase with the FCC lattice leads first, to hardening of the high-temperature phase and achievement of a high-strength state with the yield strength σ_{cr} greater than $G/100$ (G is the austenite shear modulus). Second, the γ′-phase increases the degree of tetragonality of α′-martensite, leads to the change of the strain mechanism of α′-martensite with invariant lattice from slip in the single phase state to twinning during aging and of the non-thermoelastic γ–α′ MT to thermoelastic transition with SME and SE [1–20]. Thus, precipitation of the ordered γ′-phase creates conditions for the thermoelastic γ–α′ MT in the disordered initial phase. The ordered β-phase in polycrystals of the Fe–Ni–Co–Al–X (X = Ta, Nb, and Ti) iron-based alloys precipitates along the grain boundaries with

[1]V. D. Kuznetsov Siberian Physical-Technical Institute at Tomsk State University, Tomsk, Russia; e-mail: chum@phys.tsu.ru; kireeva@spti.tsu.ru; bolga@sibmail.com; panchenko.marina4@gmail.com; [2]University of Kentucky, Lexington, USA, e-mail: karacahaluk@uky.edu; [3]University of Hannover, Hannover, Germany, e-mail: maier@iw.uni-hannover.de. Translated from Izvestiya Vysshikh Uchebnykh Zavedenii, Fizika, No. 7, pp. 16–23, July, 2015. Original article submitted March 2, 2015.

simultaneous precipitation of the γ'-phase inside the grain leading to a sharp decrease in the sample ductility and its brittle fracture. This does not allow the SME and SE in polycrystals of these alloys to be investigated [1–3]. To suppress the β-phase precipitation along the grain boundaries in polycrystals of Fe–Ni–Co–Al–X (X = Ta, Nb, and Ti) iron-based alloys, alloying with boron with small concentration C_B = 0.05 at.% is used which leads to an increase in the SE from 5 to 13% at room temperature [1–3]. The purpose of the present work is elucidation of the possibility of precipitation of the ordered β-phase in single crystals of Fe – 28% Ni – 17% Co – 11.5% Al – 2.5% Nb (Nb) and Fe – 28% Ni – 17% Co – 11.5% Al – 2.5% Nb – 0.05% B (NbB) (at.%) alloys and of the effect of β-phase particles and boron on the SME and SE during the thermoelastic γ–α' MT. Nb and NbB alloy single crystals allow higher aging temperatures T = 973 K and smaller aging times (down to 10 h) to be chosen compared to the polycrystals due to the absence of grain boundaries in them and suppression of precipitation of the β-phase along the grain boundaries. To investigate the SME and SE in Nb and NbB alloys, single crystals whose tension axis was oriented along the [001] direction were selected because of the maximal lattice strain ε_0 = 8.7% under tension for the γ–α' MT [1].

1. EXPERIMENTAL TECHNIQUE

Polycrystalline ingots of Fe – 28% Ni – 17% Co – 11.5% Al – 2.5% Nb (Nb) and Fe – 28% Ni – 17% Co – 11.5% Al – 2.5% Nb – 0.05% B (NbB) (at.%) alloys were melted in an induction furnace in an inert gas atmosphere from pure components. Nb and NbB alloy single crystals were grown by the Bridgeman method in an inert gas atmosphere. Single crystal samples shaped as double blades with sizes 12 × 2.5 × 1.5 mm were cut on an electrospark machine. The sample orientation was determined with the help of a DRON-3 diffractometer using K_α iron radiation. Single crystal samples were homogenized at T = 1550 K in helium for 10 h with subsequent water quenching at room temperature. The samples were aged at T = 973 K in a helium atmosphere. Mechanical properties of crystals were investigated using an Instron testing machine at temperatures from 180 to 573 K and strain rate of $4 \cdot 10^{-4}$ s^{-1}. The SME under loading was investigated using a special facility for thermal cycling under constant external stress and heating/cooling rate of 20 K/min. The crystal structure after aging was investigated using a Hitachi H-600 electron microscope with the accelerating voltage U = 100 kV.

2. EXPERIMENTAL RESULTS AND DISCUSSION

Electron microscopy investigations showed that γ'- and β-phase particles precipitated in Nb single crystals during aging at T = 973 K for 10 h (Fig. 1). The β-phase particles were not detected in the Nb single crystals at smaller aging times. The γ'-phase particles with $L1_2$-type ordered structure have sizes 12.5–16.5 nm and a volume fraction of 20% after aging at 973 K for 10 h. The strain contrast in the bright field image and regions of diffuse scattering around fundamental reflections in the microdiffraction patterns testify to the fact that the γ′-phase particles are coherently coupled with the matrix [9]. The β-phase particles with $B2$-type ordered structure have non-equiaxial shape, thickness d = 60–80 nm, and length l = 340–500 nm after aging at 973 K for 10 h, and their volume fraction is f = 3–5%. Unlike the γ′-phase particles, the β-phase particles are coherently coupled with the matrix, which is confirmed by the absence of the strain contrast in the dark field image (Fig. 1*d*) [21]. Hence, the Nb crystals are structurally inhomogeneous after aging and consist of γ'-phase regions with high resistance to plastic strain and β-phase regions with lower strength properties. The γ'-phase particles with size of 6.5–8 nm and volume fraction of 16% were observed in the NbB alloy single crystals during aging at T = 973 K for 10 h. The β-phase particles in the NbB single crystals were not detected with the help of the electron microscope, and hence, unlike the Nb crystals, these crystals are structurally homogeneous. Thus, an analysis of the data on the structure of the examined Nb and NbB alloy single crystals after the same procedures of aging at T = 973 K for 10 h demonstrated that boron first, slowed down the aging processes and second, suppressed the β-phase formation, by analogy with polycrystals of analogous composition [1–3].

Investigation of the temperature dependence of the electroresistance ρ(T) of the Nb and NbB crystals after aging at T = 973 K for 10 h demonstrated no changes associated with the MT in the dependence ρ(T) upon cooling down to 77 K and heating up to 400 K in the free state. Hence, the temperatures of the γ–α' MT in the Nb and NbB

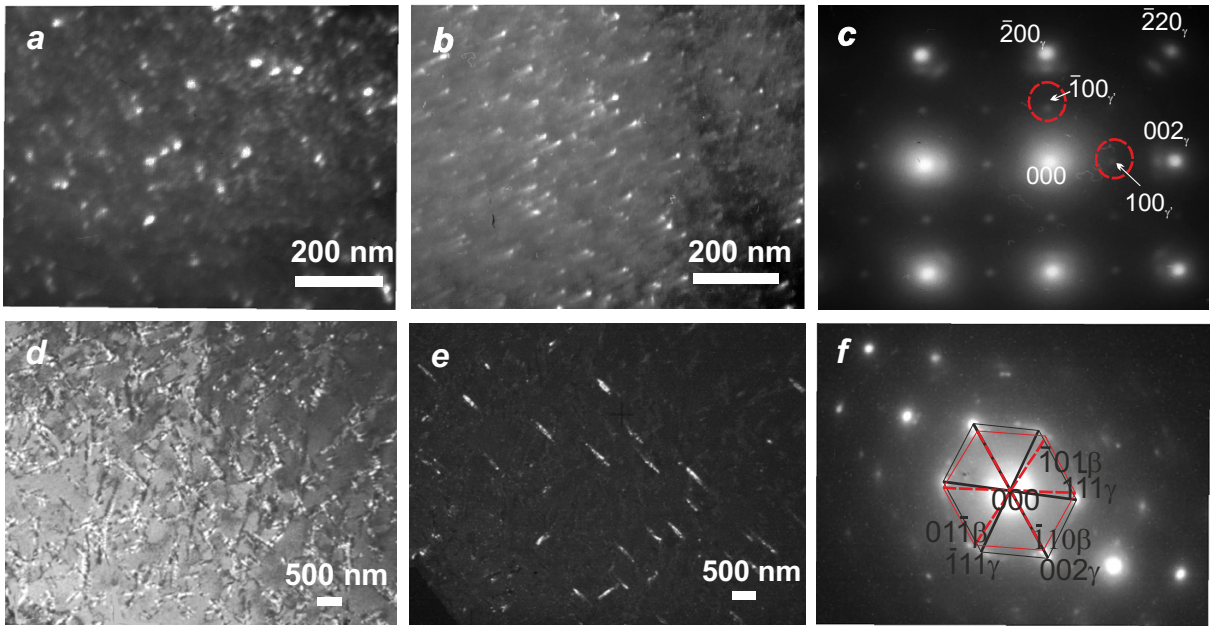

Fig. 1. Electron microscopy images of the γ′-phase particles in [001] single crystals of the alloys: *a* is for Fe – 28% Ni – 17% Co – 11.5% Al – 2.5% Nb and *b* is for Fe – 28% Ni – 17% Co – 11.5% Al – 2.5% Nb – 0.05 B (at.%) after aging at $T = 973$ K for 10 h, *c* is for microdiffraction patterns in cases *a* and *b*, and *d–f* are for the β-phase particles of [001] single crystals of the Fe – 28% Ni – 17% Co – 11.5% Al – 2.5% Nb alloy after aging at $T = 973$ K for 10 h (*d* is the bright field image, *e* is the dark field image of the β-phase particles in the particle reflection, and *c* is the diffraction pattern of single crystals after aging, $(111)_\beta \parallel (110)_\gamma$).

crystals after aging for 10 h at $T = 973$ K, by analogy with smaller aging times $t = 1$–7 h at $T = 973$ K, are lower than the liquid nitrogen temperature [8].

It was experimentally established that after aging at $T = 973$ K for 10 h, the γ–α' MT in the Nb and NbB crystals was thermoelastic, and the SME and SE were observed. Figures 2 and 3 show the results of investigations of the SME in cooling/heating experiments upon loading under external tensile stresses for the [001] Nb and NbB alloy crystals aged at 973 K for 10 h.

Precipitation of the β-phase particles in the Nb crystals and alloying of the NbB crystals with boron affect the development of the γ–α′ MT under loading. First, a maximal value of the transformation strain ε_{SME} under loading in the Nb and NbB crystals was equal to 4.0–4.2% (Fig. 2) and did not reach $\varepsilon_0 = 8.7\%$ predicted theoretically for the lattice strain of the crystals with the given orientation during the γ–α′ MT [1]. This is due to the fracture of crystals before achieving the theoretically predicted value ε_0. Second, the value of the external tensile stress σ_{ext} for the onset of the SME under loading in the NbB crystals was twice as great as that in the Nb crystals and was 500 and 250 MPa, respectively (curves *3* and *4* in Fig. 3). Third, the magnitude of thermal hysteresis ΔT^σ in the Nb crystals was constant and smaller than that in the NbB crystals, in which ΔT^σ varied with increasing σ_{ext} (curves *1* and *2* in Fig. 3).

Figure 4 shows the stress-strain curves for the [001] single crystals of Nb and NbB alloys aged at $T = 973$ K for 10 h at close values of the test temperatures under tensile strain. Figure 5 shows the dependence of the magnitude of mechanical hysteresis $\Delta\sigma$ and maximal reversible strain ε_{SE} on the test temperature of SE manifestation. It can be seen that the SE is observed in the Nb crystals at temperatures from 77 to 293 K and at temperatures from 77 to 243 K in the NbB crystals. The minimal temperatures at which the SE was detected in the Nb and NbB crystals aged at 973 K for 10 h was equal to 77 K. This confirms qualitatively that the temperatures A_f and M_s of the γ–α′ MT in the free state of the Nb and NbB crystals aged at 973 K for 10 h are smaller than 77 K, which does not contradict to the results of

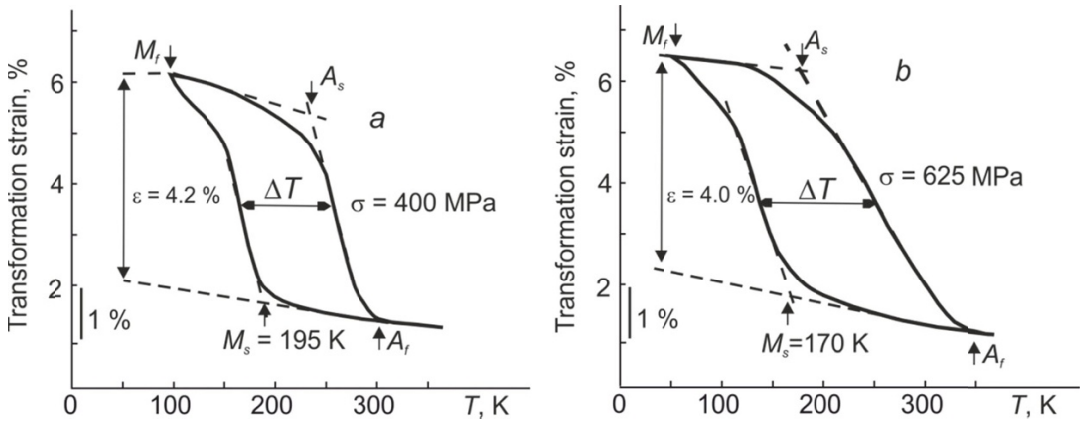

Fig. 2. Transformation strain under tensile stresses in [001] single crystals of the Fe – 28% Ni – 17% Co – 11.5% Al – 2.5% Nb (*a*) and Fe – 28% Ni – 17% Co – 11.5% Al – 2.5% Nb – 0.05 B alloys (*b*) aged at 973 K for 10 h.

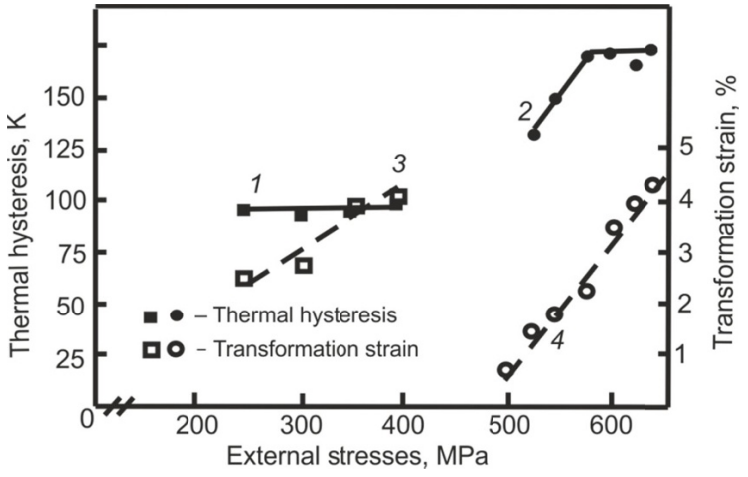

Fig. 3. Dependence of the magnitude of thermal hysteresis and of the transformation strain on the external stresses applied to the [001] single crystals of the Fe – 28% Ni – 17% Co – 11.5% Al – 2.5% Nb (curves *1* and *3*) and Fe – 28% Ni – 17% Co – 11.5% Al – 2.5% Nb – 0.05 B alloys (curves *2* and *4*) aged at 973 K for 10 h.

investigation of the dependence $\rho(T)$ in which no anomalies were detected at temperatures from 77 to 400 K. It can be seen from Figs. 4 and 5 that the presence of the β-phase particles and alloying with boron affect the γ–α′ MT under loading in the experiments on the SE investigation. First, the maximal SE ε_{SE} = 6.5% was detected in the Nb crystals; it was by a factor of 1.5 greater than that in the NbB crystals in which ε_{SE} = 4.0%. The difference between the SE values is due to the fact that the γ–α' MT in the NbB crystals under loading at the same test temperature develops under stresses σ_{cr} by a factor of 1.5 greater than those in the Nb crystals. The stresses at which the Nb crystals failed are reached in the NbB crystals under lower strains. Second, the magnitude of mechanical hysteresis Δσ determined in the middle of the SE loop increased with strain for the same test temperature (see Fig. 3) and with increasing test temperature (Fig. 5), and Δσ in the NbB crystals is greater than in the Nb crystals.

Thus, the experiments on investigation of the SME and SE under loading in the Nb and NbB crystals aged at 973 K for 10 h showed that ΔT^{σ} and Δσ in the NbB crystals are greater than in the Nb crystals. It is well known (for example, see [5–8]) that ΔT^{σ} and Δσ in single crystals of the iron-based Nb and Ta alloys aged at 973 K for 1–7 h

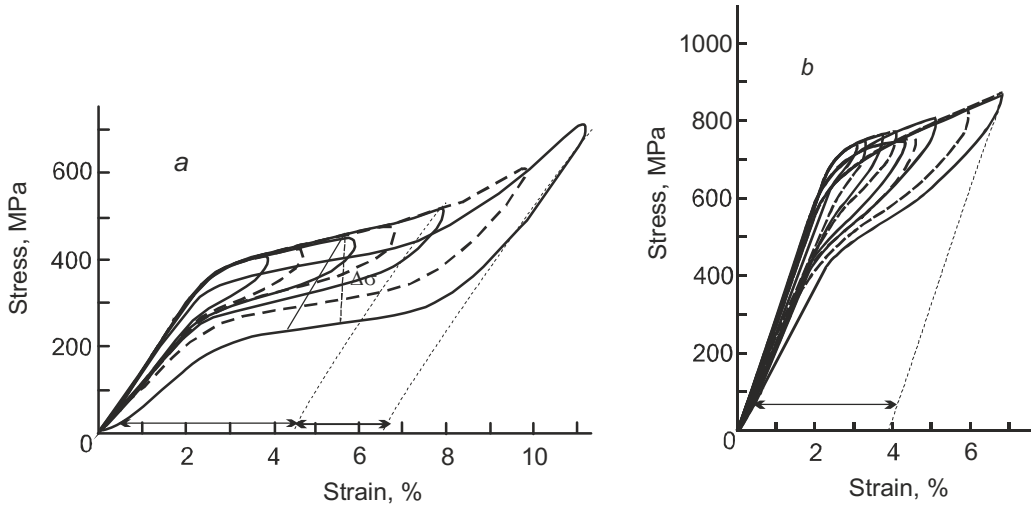

Fig. 4. Stress-strain curves for the [001] single crystals of the Fe – 28% Ni – 17% Co – 11.5% Al – 2.5% Nb alloy at T = 188 K (*a*) and of the Fe – 28% Ni – 17% Co – 11.5% Al – 2.5% Nb – 0.05 B (at.%) alloy at T = 198 K (*b*) aged at 973 K for 10 h upon tensile strain.

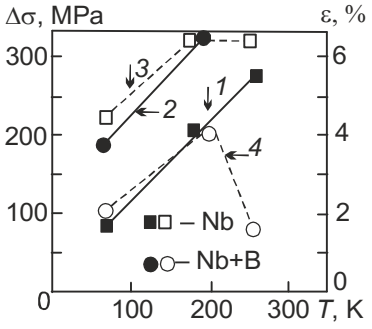

Fig. 5. Dependences of the mechanical hysteresis $\Delta\sigma$ (curves *1* and *2*) and maximal reversible strain ε_{SE} (curves *3* and *4*) on the temperature in the [001] single crystals of the Fe – 28% Ni – 17% Co – 11.5% Al – 2.5% Nb and Fe – 28% Ni – 17% Co – 11.5% Al – 2.5% Nb – 0.05 B (at.%) alloys aged at 973 K for 10 h.

depend on the strength properties of the high-temperature phase determined by the size and volume fraction of the dispersed γ'-phase particles: the smaller the size and the lower the volume fraction of the γ'-phase particles, the weaker are the strength properties of the high-temperature phase and the greater are the magnitudes of ΔT^{σ} and $\Delta\sigma$ in the experiments on investigation of the SME and SE under loading. Therefore, to elucidate the common features of the dependences obtained previously, the strength properties of the high-temperature phase and the σ_{cr} value during the γ–α' MT under loading in the Nb and NbB crystals in the single-phase state and after aging at 973 K for 10 h were investigated in a wide temperature interval from 77 to 523 K.

Figure 6 shows the temperature dependence of the stresses σ_{cr} in the Nb and NbB crystals in the single-phase state after quenching and aging at T = 973 K for 10 h at temperatures from 77 to 523 K. As can be seen from curve *1* in Fig. 6, the curve $\sigma_{cr}(T)$ in the single-phase state after quenching from 1550 K for 1 h in the Nb and NbB crystals has the normal temperature dependence characteristic for the single- and polycrystals of FCC alloys, namely, σ_{cr} decreases with increasing test temperature [22]. This qualitatively confirms that the γ–α' MT under loading in the single-phase Nb and NbB crystals at temperatures T = 77–550 K is not observed under stresses near the yield stress value, which is in

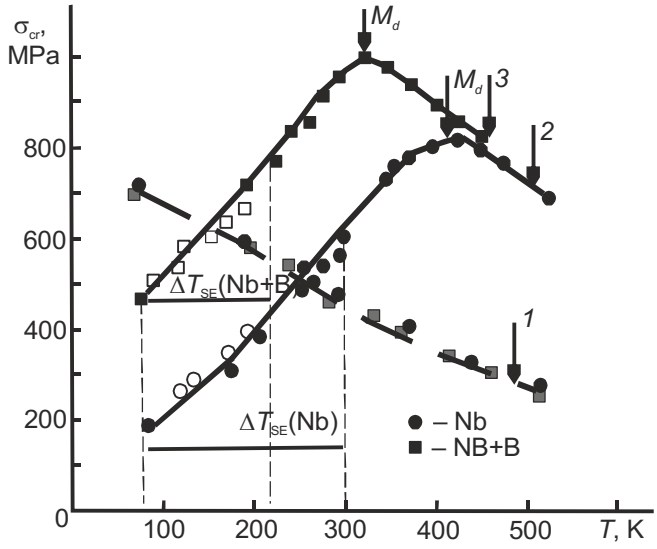

Fig. 6. Temperature dependences of the critical stresses σ_{cr} and superelasticity temperature range for the [001] single crystals of the Fe – 28% Ni – 17% Co – 11.5% Al – 2.5% Nb (curves *1* and *2*) and Fe – 28% Ni – 17% Co – 11.5% Al – 2.5% Nb – 0.05 B (at.%) alloys in the single-phase state (curves *1* and *3*) after quenching (curve *1*) and aging at 973 K for 10 h (curves *2* and *3*) under tensile strain.

agreement with the experimental data obtained in the study of the temperature dependence $\rho(T)$. After alloying with boron to 0.05 at.%, σ_{cr} in the NbB crystals became equal to that in the Nb crystals for the entire range of the examined temperatures. Hence, low concentrations of boron of the order of 0.05 at.% do not lead to solid solution hardening typically observed in the FCC single- and polycrystals at high concentrations of interstitial atoms [22].

During aging at $T = 973$ K for 10 h, the temperature dependence $\sigma_{cr}(T)$ differed from $\sigma_{cr}(T)$ for crystals in the single-phase state, and its behavior was characteristic for the alloys undergoing the MT under loading [23, 24]. When the test temperature increased from 77 to 300 and 400 K, respectively, for the Nb and NbB crystals, σ_{cr} increase was observed described by the Clapeyron–Clausius formula [23, 24]:

$$\frac{d\sigma_{cr}}{dT} = -\frac{\Delta H}{\varepsilon_0 T_0} = -\frac{\Delta S}{\varepsilon_0}. \qquad (1)$$

Here ΔH and ΔS are changes of the enthalpy and entropy, respectively, during the γ–α' MT, ε_0 is the transformation strain, and T_0 is the temperature of the chemical equilibrium of the phases. As can be seen from Fig. 6, the $\sigma_{cr}(T)$ curve is shifted in the parallel direction toward lower test temperatures during the same aging (at $T = 973$ K for 10 h) after alloying with boron compared to the Nb crystals. The curves $\sigma_{cr}(T)$ for both crystals extrapolated toward $\sigma_{cr} = 0$ showed that the M_s^0 values lie below the liquid nitrogen temperature and that $\Delta M_s^0 = M_s^0(\text{NbB}) - M_s^0(\text{Nb})$ is equal to 150 K. Hence, alloying with boron caused the austenite stabilization. Here $\alpha = d\sigma_{cr}(T)/dT = 1.8$ MPa/K is the same for the Nb and NbB crystals. Figure 6 shows the data obtained in the experiments on the investigation of the SME under loading (open squares and circles) at temperatures from 77 to 200 K. These data are in good agreement with the $\sigma_{cr}(T)$ curve and show that an increase in M_s^σ occurs with external stresses and that the value $\alpha = d\sigma/dM_s^\sigma = 1.8$ MPa/K is equal to that obtained in the study of the temperature dependence $\sigma_{cr}(T)$ at temperatures $T = 77$–300 K and 400 K, respectively, for the Nb and NbB crystals (Fig. 6) in complete agreement with Eq. (1).

Maximal stresses in the curves $\sigma_{cr}(T)$ were observed at the temperature M_d (here M_d is the temperature at which the stresses of martensite formation under loading are equal to those of the high-temperature phase flow) and, as follows from the data presented above, these stresses for the NbB crystals are higher by 200 MPa than for the Nb crystals. For

$T > M_d$, the second stage is observed in the dependence $\sigma_{cr}(T)$ associated with the strain of the high-temperature γ-phase. It can be seen that σ_{cr} decreases with increasing test temperature, as in the single-phase crystals (curve *1* in Fig. 6). Hence, investigation of the temperature dependence $\sigma_{cr}(T)$ for the Nb and NbB crystals shows that the temperature M_s for the NbB crystals is by 150 K lower, and the stresses σ_{cr} at $T = M_d$ are by 100 MPa greater than those for the Nb crystals (Fig. 6).

As demonstrated investigations of the temperature dependence $\sigma_{cr}(T)$ for the Nb and NbB single crystals, solid solution hardening by boron at low concentrations up to 0.05 at.% is equal to zero (curve *1* in Fig. 6). Hence, $\sigma_{cr}(M_d)$ will be determined only by the presence of the γ'- and β-phase particles precipitated during aging at 973 K for 10 h; moreover, it will depend on the particle size and volume fraction according to the following formula [25, 26]:

$$\sigma_{cr} = 3 \cdot G \cdot E^{3/2} (f \cdot r / b)^{1/2}. \quad (2)$$

Here G is the shear modulus of the high-temperature phase, $E = \Delta a/a$ is the discrepancy between the lattice parameters of the high-temperature phase and particle ($\Delta a = a_m - a_p$), f is the volume fraction of particles, r is the particle radius, and b is the modulus of the Burgers vector of slip dislocation. From Eq. (2) it follows that the higher f values and the larger r values, the stronger is particle hardening. Electron microscopy investigations of the structure of the Nb and NbB crystals after aging at 973 K for 10 h showed that the size and volume fraction of the γ'-phase particles for the NbB crystals were smaller than those for the Nb crystals. Hence, the stress level of the high-temperature phase for the Nb crystals should be higher than for the NbB crystals. However, the σ_{cr} value for the NbB crystals at $T = M_d$ is greater than for the Nb crystals (curves *2* and *3* in Fig. 6). Such difference in the stress levels at $T = M_d$ for the Nb and NbB crystals can be due to first, the difference between the temperatures M_s for both crystals. For the NbB crystals, the size and volume fraction of the γ'-phase particles were smaller than for the Nb crystals. As a result, changes in the chemical composition during aging of the NbB crystals compared to their initial state were smaller than for the Nb crystals and hence, the temperature M_s was lower [27]. Second, the difference between the $\sigma_{cr}(M_d)$ values for the Nb and NbB crystals can be due to the strong temperature dependence $\sigma_{cr}(T)$. Imposition of the decreasing temperature M_s on the strong temperature dependence $\sigma_{cr}(T)$ for the NbB crystals leads to an apparent increase in the stresses at $T = M_d$ for the NbB crystals compared to the Nb crystals. Indeed, $\Delta\sigma_{cr} = \sigma_{cr}(NbB) - \sigma_{cr}(WQ) = 580$ MPa for the NbB crystals, whereas $\Delta\sigma_{cr} = \sigma_{cr}(Nb) - \sigma_{cr}(WQ) = 500$ MPa for the Nb crystals (here $\sigma_{cr}(WQ)$ denotes stresses of the high-temperature phase for the Nb and NbB crystals after quenching, and $\sigma_{cr}(Nb)$ and $\sigma_{cr}(NbB)$ denote stresses in the Nb and NbB crystals, respectively, at $T = M_d$ after aging at 973 K for 10 h) (Fig. 6). For the NbB crystals, the $\Delta\sigma_{cr}$ value was by 80 MPa greater than for the Nb crystals. In its pure form, hardening of the high-temperature phase in the Nb and NbB crystals during aging at 973 K for 10 h can be determined at the test temperature, which is above M_d, for example 423 K, and, as can be seen from Fig. 6, $\sigma_{cr}(NbB) > \sigma_{cr}(Nb)$ by 20 MPa. For the Nb crystal aged at $T = 973$ K for 5 h and the NbB crystal aged at $T > M_d$, on the contrary, $\sigma_{cr}(NbB) < \sigma_{cr}(Nb)$. Investigation of the structure of the Nb and NbB crystals after aging at 973 K for 5 h demonstrated that the size and the volume fraction of the γ'-phase particles in the Nb crystals were also greater than in the NbB crystals, but no β-phase was observed. Hence, an insignificant increase in σ_{cr} of the high-temperature phase in the NbB crystals after aging at 973 K for 10 h compared to the Nb crystals was due to the presence of the β-phase particles whose strength properties were weaker than those of the γ'-phase. As a result, the onset of the plastic flow in the structurally inhomogeneous Nb crystals in the high-temperature phase was determined by regions near the β-phase particles, which leads to lower σ_{cr} value at $T > M_d$ compared to the structurally homogeneous NbB crystals in which the β-phase particles are absent at the same aging times, and the properties of the high-temperature phase are slightly stronger even for smaller values of the size and volume fraction of the γ'-phase particles. Hence, the β-phase particles lead to weakening of the high-temperature phase. However, the presence of the β-phase particles does not affect the magnitudes of ΔT^{σ} and $\Delta\sigma$ in the experiment on the investigation of the SME and SE under loading. The size and volume fraction of the γ'-phase particles in the Nb crystals were greater than those in the NbB crystals, whereas the magnitudes of ΔT^{σ} and $\Delta\sigma$, on the contrary, were smaller, as was the case for the crystals of iron-based alloys with a larger size and a higher volume fraction of the γ'-phase particles [5–8].

CONCLUSIONS

1. On the example of the single crystals of the Fe – 28% Ni – 17% Co – 11.5% Al – 2.5% Nb (at.%) alloy it has been shown that the precipitation of incoherent β-phase particles of non-equiaxial shape with the thickness $d = 60–80$ nm, the length $l = 340–500$ nm, and the volume fraction 3–5% in the crystal volume does not lead to embrittlement of the crystals. Moreover, the shape memory effect of 4.2% and the superelasticity up to 6.5% during the thermoelastic γ–α'-martensitic transformation were observed at temperatures from 77 to 293 K.

2. For the single crystals of the Fe – 28% Ni – 17% Co – 11.5% Al – 2.5% Nb – 0.05% B (at.%) alloy it was established that doping by boron stabilized the high-temperature phase, suppressed the formation of the β-phase, and slowed down aging processes. The shape memory effect and superelasticity of 4.0% during the thermoelastic γ–α'-martensitic transformation were observed in single crystals with boron.

3. It was experimentally shown that the temperature dependences of the stresses of the onset of the martensitic transformations under loading in single crystals of the Fe – 28% Ni – 17% Co – 11.5% Al – 2.5% Nb alloy without boron and with boron are described by the Clapeyron–Clausius formula, $\alpha = d\sigma_{cr}/dT$ is equal to 1.8 MPa/K, and boron does not affect $\alpha = d\sigma_{cr}/dT$.

4. It was experimentally shown that magnitudes of thermal hysteresis ΔT^{σ} and of mechanical hysteresis $\Delta\sigma$ under loading in crystals with boron were greater than in crystals without boron due to the effect of boron on the decrease of the temperature M_s and slowing down of the aging process.

This work was supported in part by the Russian Scientific Fund (Project No. 14-29-00012).

REFERENCES

1. Y. Tanaka, Y. Himuro, R. Kainuma, *et al*., Science, **327**, 1488–1490 (2010).
2. T. Omori, K. Ando, M. Okano, *et al.*, Science, **333**, 68–71 (2011).
3. D. Lee, T. Omori, and R. Kainuma, J. Alloys Comp., **617**, 120–123 (2014).
4. Y. Geng, D. Lee, X. Xu, *et al*., J. Alloys Comp., **628**, 287–292 (2015).
5. I. V. Kireeva, Yu. I. Chumlyakov, V. A. Kirillov, *et al*., Russ. Phys. J., **53**, No. 10, 1103–1106 (2011).
6. I. V. Kireeva, Yu. I. Chumlyakov, V. A. Kirillov, *et al*., Tech. Phys. Let., **37**, No. 5, 487–490 (2011).
7. Yu. I. Chumlyakov, I. V. Kireeva, E. Yu. Panchenko, *et al*., Russ. Phys. J., **54**, No. 8, 937–950 (2012).
8. Yu. I. Chumlyakov, I. V. Kireeva, O. A. Kuts, *et al*., Russ. Phys. J., **57**, No. 10, 1328–1335 (2015).
9. V. V. Kokorin, Martensitic Transformation in Inhomogeneous Solid Solutions [in Russian], Naukova Dumka, Kiev, 1987.
10. L. P. Gun'ko, G. A. Takazei, and A. N. Titenko, Phys. Met. Metallography, **91**, No. 6, 624–628 (2001).
11. E. Hornbogen and N. Jost, J. Physique IV, Colloque C4, Supplement an J. de Physique, **III**, No. 11, C4-199–C4-210 (1991).
12. E. Hornbogen, in: Proc. Int. Conf. on Martensitic Transformations, The Japan Institute of Metals (1986), pp. 453–458.
13. H. Y. Yasuda, M. Aoki, A. Takaoka, *et al*., Scripta Mat., **53**, 253–257 (2005).
14. T. Maki, Shape Memory Materials, K. Otsuka and C. M. Wayman, eds., Cambridge University Press, United Kingdom (1998).
15. H. Sehitoglu, C. Efstathion, H. J. Maier, and Y. Chumlyakov, Mech. Mater., **38**, 538–550 (2006).
16. H. Sehitoglu, X. Y. Zhang, T. Kotil, D. Canadic, *et al*., Metallurg. Mater. Trans., **33A**, 3661–3672 (2002).
17. A. Evirgen, J. Ma, I. Karaman, *et al*., Scripta Mat., **67**, 475–478 (2012).
18. J. Ma, B. Kockar, A. Evirgen, *et al*., Acta Mat., **60**, 2186–2195 (2012).
19. J. Ma, B. C. Hombuckle, I. Karaman, *et al*., Acta Mat., **61**, No. 9, 3445–3455 (2013).
20. P. Kroos, T. Niendorf, I. Karaman, *et al*., Funct. Mater. Lett., **5**, No. 5, 1250045 (4 pp.) (2012).
21. P. Khirsh, A. Khovi, R. Nikolson, *et al.*, Electron Microscopy of Thin Crystals [Russian translation], Mir, Moscow (1968).
22. Yu. I. Chumlyakov, I. V. Kireeva, A. D. Korotaev, *et al*., Russ. Phys. J., **39**, No. 3, 189–210 (1996).

23. K. Otsuka and X. Ren, Prog. Mater. Sci., **50**, No. 5, 511–678 (2005).
24. K. Otsuka, A. Saxena, J. Deng, *et al*., Phil. Mag., **91**, No. 36, 4514–4535 (2011).
25. E. Nembach, Particle Strengthening of Metals and Alloys, John Wiley & Sons, Inc., New York; Chichester; Brisbane; Toronto; Singapore; Weinheim (1997).
26. M. F. Ashby, Phil. Mag., **21**, 399–424 (1970).
27. E. Hornbogen, V. Mertinger, and D. Wurzel, Scripta Mater., **44,** 171–178 (2001).